applied optics

Least squares method for liquid crystal display characterization

Dafne Amaya,[1] Daniel Actis,[1] Gonzalo Rumi,[1] and Alberto Lencina[2,*]

[1]Centro de Investigaciones Ópticas, CONICET-UNLP-CIC, P.O. Box 3, 1897 Gonnet, Argentina
[2]Laboratorio de Análisis de Suelos, Facultad de Agronomía, Universidad Nacional del Centro de la Provincia de Buenos Aires, CONICET, P.O. Box 47, 7300 Azul, Argentina
*Corresponding author: alencina@faa.unicen.edu.ar

Received 24 May 2016; revised 19 September 2016; accepted 17 January 2017; posted 17 January 2017 (Doc. ID 266918); published 8 February 2017

This paper presents a method for liquid crystal display characterization. It assumes a liquid crystal display can be considered as a polarization-changing device described by a Jones matrix plus a global phase. The Jones matrix parameters are found by a least squares minimization based on global optimization techniques. The present method avoids the need for assigning experimental values to theoretical expressions, and it is robust against intensity fluctuations, does not require arbitrarily fixing any sign of the parameters estimated, and only one quarter-wave plate is employed. A comparative analysis of the results obtained with this method and previous ones is performed. Having completely characterized a liquid crystal display, a phase-mostly configuration is obtained and experimentally verified. © 2017 Optical Society of America

OCIS codes: (230.6120) Spatial light modulators; (230.3720) Liquid-crystal devices; (050.1970) Diffractive optics.

https://doi.org/10.1364/AO.56.001438

1. INTRODUCTION

Spatial light modulators based on liquid crystal displays (LCDs) have presently gained a place in most optic and laser laboratories. They are used in several branches of research, such as atomic physics [1], quantum optics [2], speckle pattern generation [3,4], optical vortices [5,6], and beam shaping [7,8], among others [9]. In the case of twisted nematic LCDs (TN-LCDs), owing to the fact that light polarization is changed, they must be complemented with polarizers and quarter-wave plates to allow amplitude or phase modulation. These polarizers and quarter-wave plates must be set according to the TN-LCD characteristics. However, it is usual that specifications provided by manufacturers are insufficient to use them in a phase-mostly configuration. Due to this, to maximize their use, it is necessary to perform a proper TN-LCD characterization.

Several methods have been developed to achieve a suitable characterization of LCDs. They can be classified into two groups: (1) a model for the liquid crystal molecules is developed and the internal parameters are obtained [10–13], and (2) the LCD is considered as a polarization-changing device and its macroscopic parameters are searched for [14–18]. The first group suffers from the drawback that all LCDs are different and not necessarily all models can be applied to any LCD, nor is it known *a priori* which model must be employed for a specific model. On the other hand, the developments of the second group have a practical point of view, where the parameters required to properly configure a SLM are obtained, regardless of how the LCD behaves internally. In that sense, this group has the advantage that all methods can be applied to any LCD.

Among the methods of the second group, that proposed by Moreno *et al.* [14] is distinguished by its operational approach to the problem: it considers that the LCD can be described by a unitary matrix and a global phase. Based on seven intensity measurements, the four parameters of the unitary matrix are obtained. An additional interferometric measurement allows one to obtain the global phase. Afterwards, Ma *et al.* [15] improved the method by reducing the intensity measurements to only three. However, these methods have some drawbacks. Both directly assign an experimental value, which is intrinsically subject to an error, to a theoretical expression of a model. A better option would be to obtain a *best estimator* of the theoretical value via an optimization procedure. Moreover, both are unstable against intensity fluctuations; the Baiheng Ma method needs to arbitrarily assign the relative signs of the parameters; and some measurements require the use of two quarter-wave plates, increasing the required equipment and possibly introducing more aberrations and alignment issues to the system.

In this paper, we present a method to determine the Jones matrix of any nonabsorbing polarization-changing device. The present method solves the discussed drawbacks in characterizing TN-LCD and can be applied to others LCDs, such as

reflective PA-LCoS and TN-LCoS displays. A total of eight normalized intensity measurements described in terms of laboratory angles are needed to apply our method. Some of them require at most only one quarter-wave plate (QWP), which is always placed before the LCD. In this sense, the method is expressed in an amenable language for the experimental researcher and minimizes the need for duplicated accessories not always found in all laboratories. Following the intensity measurements, and based on a global least squares minimization, the best estimators for the LCD parameters are found. In this way, the assignment of experimental measurements to theoretical expressions is avoided. At the same time, the estimators are robust against intensity fluctuations. Besides, the fitting procedure eliminates the need to select the relative signs of the parameter estimators. In short, although this method requires more measurements than others (due to the nonlinearity of the equations), it resolves misconceptions, is robust to fluctuations, and requires less laboratory tools.

The paper is organized as follows. In Section 2, the previous methods are revisited and their strengths and drawbacks are highlighted. In Section 3, the least squares method is proposed and the details of its implementation are given, while Section 4 comparatively presents the results of the experimental implementation of the methods. A complete characterization of our TN-LCD LC2002 from Holoeye is presented in Section 5, where the global phase is determined. To verify the correctness of the method, a phase-mostly implementation with our LC2002 is presented in Section 6. Finally, the conclusions are established in Section 7.

2. REVIEW OF PREVIOUS METHODS

In this section, a review of the main aspects of the Moreno *et al.* [14] and Ma *et al.* [15] methods is carried out. The focus is placed on intensity measurements where the differences between the methods appear. The description of the model for the LCD, the equations that describe its behavior, and the way its parameters are measured are detailed. The advantages and disadvantages of each method are highlighted.

A. Moreno Method [14]

In 2003, Moreno presented a method for LCD characterization based on a Jones matrix. There, "the macroscopic action of the LCD on the polarization state is evaluated, but no assumption is made about the microscopic physical parameters that determine this effect." In this sense, the LCD is considered as a nonabsorbing display described by a unitary Jones matrix plus a global phase. The four real-valued elements of the matrix are determined through intensity measurements, and the global phase is interferometrically obtained.

The setup employed for intensity measurements is shown in Fig. 1. A laser-emitting circularly polarized light is spatially filtered by a spatial filter SF and collimated by lens L_1. This beam impinges on a polarization state generator (PSG) (composed of polarizer P_1 and quarter-wave plate QWP_1). The resulting polarized light passes through the LCD and a polarization state detector (PSD) (composed of quarter-wave plate QWP_2 and polarizer P_2), and lens L_2 focuses it onto a microscope objective MO, being detected afterward by a CCD.

After the PSG, the light can be described by the Jones vector (in Dirac *bra-ket* notation)

$$|\chi,\phi\rangle = \begin{pmatrix} \cos(\chi) \\ \sin(\chi)\exp(j\phi) \end{pmatrix}, \tag{1}$$

where $0 \le \chi \le \pi/2$ is the angle which defines the relative weight between the components of the vector, and $0 \le \phi \le 2\pi$ is its phase difference. The LCD is described by a 2×2 unitary matrix

$$M = c\,\exp(-j\beta)\begin{pmatrix} X-jY & Z-jW \\ -Z-jW & X+jY \end{pmatrix}, \tag{2}$$

being c a constant representing the intensity loss caused by surface reflections, etc. and β a global phase shift. The parameters X, Y, Z, and W are real values in the range $[-1, 1]$ that satisfy the normalization condition $X^2+Y^2+Z^2+W^2=1$. Finally, the effect of the PSD is described by the *bra* $\langle\chi,\phi|$. Then, the intensity detected by the CCD is given by

$$I = |\langle\chi_2,\phi_2|M|\chi_1,\phi_1\rangle|^2. \tag{3}$$

Within this framework, the measurement of the transmitted intensity for seven different configurations of the PSG and the PSD are considered for the calibration procedure. The normalized transmitted intensity is measured as a function of the addressed gray level, obtaining the curves $I_i(g)$, $i=1,2\ldots7$. Moreno selected the following seven configurations:

$$I_1 = |\langle 0,0|M|0,0\rangle|^2 = X^2+Y^2, \tag{4a}$$

$$I_2 = \left|\left\langle \frac{\pi}{2},0\middle|M\middle|0,0\right\rangle\right|^2 = Z^2+W^2, \tag{4b}$$

$$I_3 = \left|\left\langle \frac{\pi}{4},\frac{3\pi}{2}\middle|M\middle|0,0\right\rangle\right|^2 = \frac{1}{2}(X+W)^2+\frac{1}{2}(Y+Z)^2, \tag{4c}$$

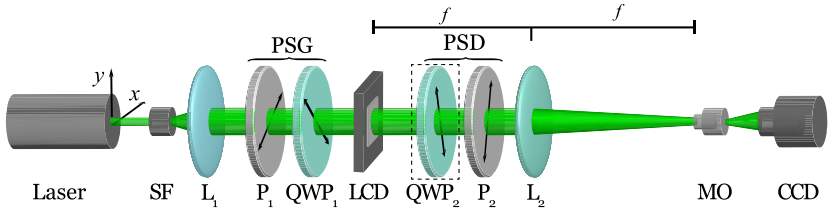

Fig. 1. Experimental setup for XYZW determination. A laser is passed through by a spatial filter SF and collimated by lens L_1. This beam impinges on a PSG (composed of polarizer P_1 and quarter-wave plate QWP_1). The resulting polarized light passes through the LCD and a PSD (composed of quarter-wave plate QWP_2 and polarizer P_2) and lens L_2 focuses it onto a microscope objective MO and is detected by a CCD. The dashed lines around QWP_2 indicate that it is used in some cases and not in others.

$$I_4 = \left|\left\langle \frac{\pi}{2}, 0 \middle| M \middle| \frac{\pi}{4}, \frac{\pi}{2} \right\rangle\right|^2 = \frac{1}{2}(Z+Y)^2 + \frac{1}{2}(X-W)^2, \tag{4d}$$

$$I_5 = \left|\left\langle 0, 0 \middle| M \middle| \frac{\pi}{4}, 0 \right\rangle\right|^2 = \frac{1}{2}(X+Z)^2 + \frac{1}{2}(Y+W)^2, \tag{4e}$$

$$I_6 = \left|\left\langle \frac{\pi}{2}, 0 \middle| M \middle| \frac{\pi}{4}, 0 \right\rangle\right|^2 = \frac{1}{2}(X-Z)^2 + \frac{1}{2}(Y-W)^2, \tag{4f}$$

$$I_7 = \left|\left\langle \frac{\pi}{4}, 0 \middle| M \middle| 0, 0 \right\rangle\right|^2 = \frac{1}{2}(X-Z)^2 + \frac{1}{2}(Y+W)^2. \tag{4g}$$

From these measurements, the $XYZW$ parameters are obtained as

$$X^2 = \frac{I_1}{1 + \left(\frac{I_7 - I_6}{I_3 - I_4}\right)^2}, \tag{5a}$$

$$Y^2 = \frac{I_1}{1 + \left(\frac{I_3 - I_4}{I_7 - I_6}\right)^2}, \tag{5b}$$

$$Z^2 = \frac{I_2}{1 + \left(\frac{I_3 - I_4}{I_5 - I_7}\right)^2}, \tag{5c}$$

$$W^2 = \frac{I_2}{1 + \left(\frac{I_5 - I_7}{I_3 - I_4}\right)^2}. \tag{5d}$$

The previous results must be complemented with the relative signs among the parameters. Assuming $\mathrm{sign}[X] = +1$, the remaining signs are determined from

$$\mathrm{sign}(Z) = \frac{\mathrm{sign}(I_5 - I_7)}{\mathrm{sign}(X)}, \tag{6a}$$

$$\mathrm{sign}(W) = \frac{\mathrm{sign}(I_3 - I_4)}{\mathrm{sign}(X)}, \tag{6b}$$

$$\mathrm{sign}(Y) = \frac{\mathrm{sign}(I_7 - I_6)}{\mathrm{sign}(W)}. \tag{6c}$$

This method, in comparison with those that obtain the internal parameters of the LCD, has the following advantages: (1) it does not require a previous calibration of the LCD internal microscopic parameters, (2) only one wavelength is required, (3) no assumptions are made about the liquid crystal orientation as a function of the voltage, (4) the laboratory reference frame can be employed, and (5) it can be employed not only for twisted nematic LCDs but also for any other nonabsorbing linear polarization display that can be described by a Jones matrix. On the other hand, the main disadvantage is related to its sensibility to intensity fluctuations, which translates into a high instability to calculate the $XYZW$ parameters from Eqs. (5) and (6). This is a consequence of assigning experimental results to theoretical ones [Eq. (4)]. Additionally, the sign of X must be arbitrarily fixed for all the gray level values. Finally, although Moreno claims that only one QWP is needed, a circularly polarized incident beam is employed, which requires another QWP.

B. Baiheng Ma Method [15]

Several years later, in 2010, Baiheng Ma introduced an improved version of the previous method, considerably diminishing the number of intensity measurements required to determine the $XYZW$ parameters. Considering the same modeling for the LCD and the same experimental setup, the proposed measurements are the following:

$$I_1' = |\langle 0, 0|M|0, 0\rangle|^2 = X^2 + Y^2, \tag{7a}$$

$$I_2' = \left|\left\langle \frac{\pi}{4}, \frac{\pi}{2} \middle| M \middle| \frac{\pi}{4}, \frac{3\pi}{2} \right\rangle\right|^2 = X^2 + Z^2, \tag{7b}$$

$$I_3' = \left|\left\langle \frac{\pi}{4}, 0 \middle| M \middle| \frac{\pi}{4}, 0 \right\rangle\right|^2 = X^2 + W^2. \tag{7c}$$

By properly combining these measurements, the $XYZW$ parameters are obtained from

$$X^2 = \frac{1}{2}(I_1' + I_2' + I_3' - 1), \tag{8a}$$

$$Y^2 = \frac{1}{2}(I_1' - I_2' - I_3' + 1), \tag{8b}$$

$$Z^2 = \frac{1}{2}(I_2' - I_1' - I_3' + 1), \tag{8c}$$

$$W^2 = \frac{1}{2}(I_3' - I_1' - I_2' + 1). \tag{8d}$$

Then, the main advantage of this method is to reduce from seven to three the number of intensity measurements needed to calculate the $XYZW$ parameters. However, although nothing is said about the relative signs assignment, it is known that they must arbitrarily be assigned as "+," "+," "-," and "-" for $XYZW$, respectively [19]. Moreover, this method suffers from the same drawback as the previous one: it directly assigns an experimental value to a theoretical expression of a model. This translates into a difficulty in calculating values that are close to zero in the presence of the intensity fluctuations. Finally, although the first and the third measurements do not require a QWP, the second one must be carried out with two QWPs.

3. LEAST SQUARES METHOD

As discussed in the previous sections, there are three common drawbacks to the methods proposed by Moreno and Baiheng Ma: the instability in presence of intensity fluctuations (a direct consequence of the assignment of experimental results to theoretical models), the need for arbitrarily setting at least one of the signs of the determined parameters, and the requirement of more than one QWP. Therefore, in this section, we present a method based on least squares minimization to obtain the best estimator of the $XYZW$ parameters while avoiding all of the above-mentioned drawbacks.

As a first step, consider the experimental setup shown in Fig. 1 where only QWP_1 is employed. Next, the incident laser is assumed vertically polarized. Then, instead of using the Dirac *bra-ket* notation, we prefer to describe the measured intensity in

terms of the angles of the optical components with respect to the horizontal axis of the laboratory (being the positive angles if rotating counterclockwise when the observer is looking in the opposite direction of the propagation of the light beam). With these considerations, the intensity measured by the CCD is given by

$$\begin{aligned} I(\theta_1,\phi,\theta_2) = {} & \frac{c}{2}(X\cos(\theta_1-\theta_2)-Y\cos(\theta_1-\theta_2-2\phi) \\ & +Z\sin(\theta_1-\theta_2)+W\sin(\theta_1-\theta_2-2\phi))^2 \\ & +\frac{c}{2}(X\cos(\theta_1+\theta_2-2\phi)+Y\cos(\theta_1+\theta_2) \\ & -Z\sin(\theta_1+\theta_2-2\phi)+W\sin(\theta_1+\theta_2))^2, \end{aligned} \tag{9}$$

where c has the same meaning as in Eq. (2), θ_i is the angle of the polarizer P_i, and ϕ is the angle of QWP_1.

Based on the considered setup, a total of eight angle combinations are proposed to be measured for the LCD characterization. From Eq. (9), the (normalized) proposed measurements are as follows:

$$I_1''\left(\frac{\pi}{2},\frac{\pi}{2},\frac{\pi}{2}\right) = X^2+Y^2, \tag{10a}$$

$$I_2''\left(\frac{\pi}{2},\frac{\pi}{2},\frac{7\pi}{4}\right) = \frac{1}{2}+WY-XZ, \tag{10b}$$

$$I_3''\left(\frac{3\pi}{4},\frac{\pi}{2},0\right) = \frac{1}{2}+WX-YZ, \tag{10c}$$

$$I_4''\left(\frac{3\pi}{4},\frac{\pi}{2},\frac{\pi}{4}\right) = \frac{1}{2}-XY-WZ, \tag{10d}$$

$$I_5''\left(\frac{\pi}{4},\frac{\pi}{4},\frac{\pi}{4}\right) = X^2+W^2, \tag{10e}$$

$$I_6''\left(\frac{\pi}{4},\frac{\pi}{4},0\right) = \frac{1}{2}+WY+XZ, \tag{10f}$$

$$\begin{aligned} I_7''\left(\frac{\pi}{2},\frac{\pi}{6},\frac{\pi}{2}\right) = {} & \frac{1}{8}\left(2X-Y-\sqrt{3}W\right)^2 \\ & +\frac{1}{8}\left(X+2Y+\sqrt{3}Z\right)^2, \end{aligned} \tag{10g}$$

$$\begin{aligned} I_8''\left(\frac{\pi}{2},\frac{\pi}{3},\frac{\pi}{2}\right) = {} & \frac{1}{8}\left(2X+Y-\sqrt{3}W\right)^2 \\ & +\frac{1}{8}\left(2Y-X+\sqrt{3}Z\right)^2, \end{aligned} \tag{10h}$$

where it was explicitly assumed that $X^2+Y^2+Z^2+W^2=1$.

Because all experimental measurements entail intensity fluctuations and other contributions from random errors, it is incorrect to "equalize" the resulting intensity expressions from Eq. (9) to their corresponding experimental measurements. Considering this, it can only be asserted that there may be a set of parameters $XYZW$ that best describes the results of the experimental measurements. This approach circumvents the direct assignment of experimental values to a theoretical expression of a model.

Based on the assumption that intensity measurements are statistically independent and their errors are of Gaussian distribution [20], the following estimator can be proposed to find the set of parameters to be determined:

$$\text{Est} = \sum_{i=1}^{8}(I_i''-I_i^e)^2, \tag{11}$$

where I_i^e is the measured intensity when the angles corresponding to I_i'' [Eq. (10)] are set. By minimizing Est, the best estimated parameters $XYZW$ are found. This minimization has to be performed for each gray level. To avoid the need for carefully setting the initial values of the minimization procedure (due to the risk of falling down in local minima), a global optimization algorithm is employed. The Nelder–Mead method [21] included in the `NMinimize` package of Wolfram Mathematica [22] is used (a Wolfram Mathematica implementation of the least squares method employed in this work can be downloaded from [23]).

The purpose of Eq. (11) is to deal correctly with the experimental results to estimate the $XYZW$ parameters. Moreover, this method is intrinsically robust against intensity fluctuations and avoids the need for arbitrarily fixing the relative signs of $XYZW$. Besides, only one QWP (always before the LCD) is used. In the next section, this method and the previous ones are comparatively analyzed.

4. EXPERIMENTAL RESULTS

In this section, the three previously mentioned methods are experimentally evaluated. To do this, the setup of Fig. 1 was implemented. The list of components was as follows: a doubled Nd:YAG laser (Compass 315M-150, $\lambda = 532$ nm) from Coherent, a spatial filter [910A, with a pinhole (910PH-5, 5 μm), and a microscope objective (M-20 ×, 20 ×)] from Newport, a collimating lens (45-169, focal length 20 cm, diameter 50.8 mm) from Edmund Optics, two polarizers (03FPG007) mounted in manual rotation mounts (07HPR003, 1° minimum scale; 07HPT735, 0.1° minimum scale) each from Melles Griot, one multiple-order quarter wave-plate (05RP14-16) mounted in a manual rotatory stage (RSP-1T, 2° minimum scale) both from Newport, a Berek polarization compensator (5540, 0.4° minimum scale) from New Focus adjusted for quarter-wave plate operation at $\lambda = 532$ nm, a TN-LCD (LC2002, 8 bits gray levels) from Holoeye, a lens (LB-1199, 20 cm focal length) from Thorlabs, and a DIN microscope objective (39339, 20 ×) from Edmund Optics coupled to a CCD camera (DCU224M, monochrome, 8 bits) from Thorlabs. The LCD control and acquisition were carried out with a homemade MATLAB routine. The average of the central region (40 pixels × 40 pixels) of the light spot is considered as the intensity measurement. This ensures that intensity is measured with a relative error-of-the-mean lesser than 1%. The LCD gray levels were varied in steps of five, giving a total of 52 measurements. To remove the influence of the c constant from all methods, the complementary intensity (by rotating the last polarizer 90°) was acquired and employed to normalize the measured intensity. The data

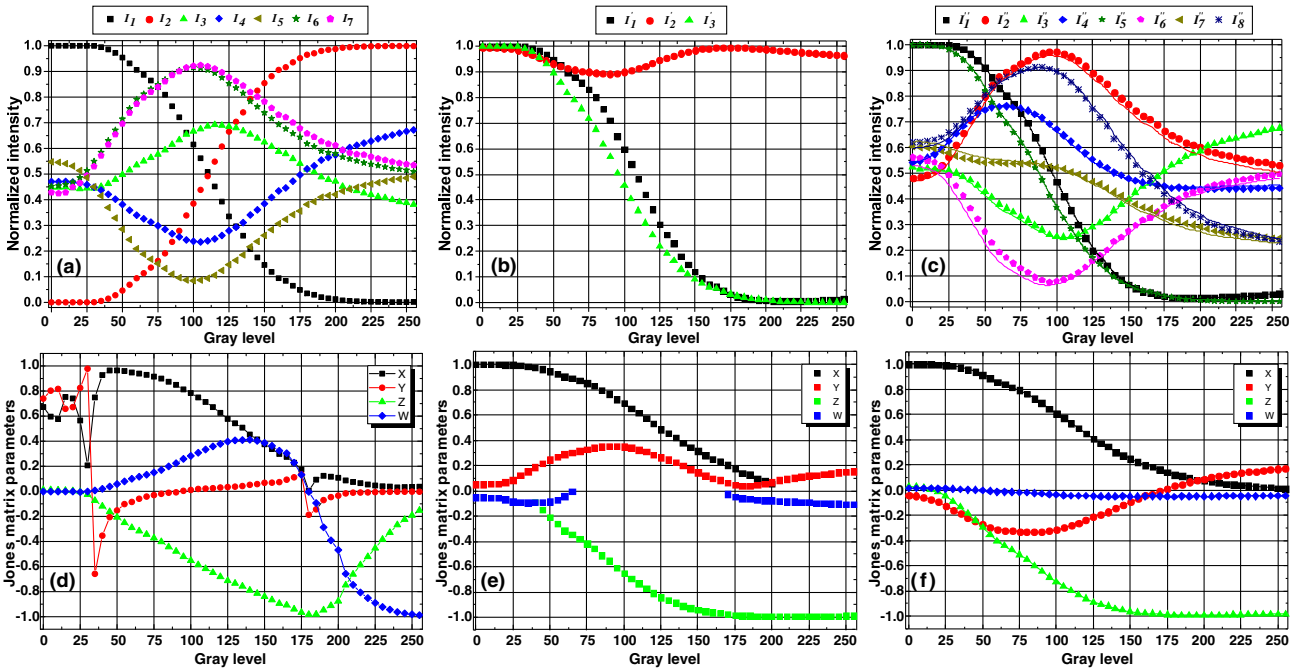

Fig. 2. Measured intensities (a)–(c) employed to determine $XYZW$ (d)–(f) for each model: (a),(d) Moreno; (b),(e) Baiheng Ma; and (c),(f) least squares.

processing was performed with Origin for the Moreno and the Baiheng Ma methods. Wolfram Mathematica was employed for the least squares method [23]. Although it seems too demanding, the least squares method takes less than 1 min to determine the $XYZW$ for all gray levels in a 3 GHz CPU.

The measured intensities for the Moreno method, the Baiheng Ma method, and the least squares method are depicted in Figs. 2(a)–2(c), respectively, and the obtained $XYZW$ values for each method are shown in Figs. 2(d)–2(f), respectively.

From Fig. 2(a), it can be seen that all measurements cross at least one time. These crossings led to the abrupt peaks and sign changes in the $XYZW$ determination, as is apparent in Fig. 2(d). On the other hand, when the measurements displayed in Fig. 2(b) are employed to calculate the $XYZW$ parameters, nonreal values appear, leaving them undetermined for several gray levels, as is visible in Fig. 2(e). These results clearly show the issue concerning the intensity fluctuations that results in very pronounced instabilities in the $XYZW$ determination. A detailed analysis of these results is given in Appendix A.

Figure 2(c) shows the eight intensity measurements (dots) proposed in Eq. (10). From the figure it is apparent that almost all measurements have a distinct behavior as a function of the gray level displayed in the LCD. Note that although several of them intersect at one gl, there are others that do not. This fact helps the least squares algorithm to properly identify the correct contribution of each $XYZW$ for each gray level. The result of minimizing Est from Eq. (11) is displayed in Fig. 2(f). The estimated $XYZW$ values are smooth curves and for each gray level satisfies $X^2 + Y^2 + Z^2 + W^2 = 1$.

The predictive capability of the estimated parameters is tested by calculating the eight intensity measurements, as shown by the continuous lines in Fig. 2(c). Although there are small differences between measured and calculated results, they can be attributed to the precision of the optical components [poor precision for QWP positioning, few intensity digitalization levels (8 bits), etc.,] used in our experimental setup. In that sense, this lack of precision can also be considered as a source of intensity fluctuations. Then, the results show that the least squares method is very robust against intensity fluctuations. Besides, it does not need to arbitrarily assign the relative signs of $XYZW$.

At this point, a comment in relation to the depolarization needs to be made. There are several works devoted to the measurement of the Mueller matrices to take into account depolarization [24,25]. It appears due to the flickering of the voltage addressed to the liquid crystal molecules, which in turn leads to a varying polarization that is incoherently time-averaged by the detector. Obtained values of the degree of depolarization are, in general, lower than 10%. Within this range, and assuming the polarized light is in the interval [0,1], the error introduced in a normalized intensity measurement is lower than 5% when the polarized light tends to zero or one and approaches 0% for light around 0.5 (see Appendix B for details). Then, if the proposed measurements are uniformly distributed around 0.5, the error in the least squares method coming from depolarization is compensated, being minimized if the measurement is close to 0.5. Thus, the least squares method is also robust against intensity fluctuations coming from depolarization. Anyway, from Figs. 2(a)–2(c), it is clear that depolarization it is not a significant issue in our device because there is no background (unpolarized) intensity measured.

Before ending this section, some words need to be said about Eq. (10): this is not the only set of measurements that

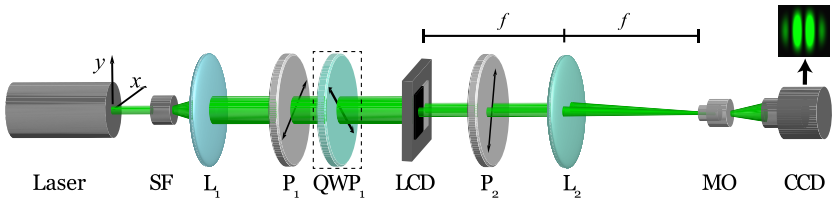

Fig. 3. Experimental setup for β determination. A laser is passed through a spatial filter SF and collimated by lens L_1. This beam impinges on polarizer P_1 and then on quarter-wave plate QWP_1. The resulting polarized light passes through the LCD, which has a pupil with two holes. On one hole the gray level is fixed, whereas on the other it is varied. The two beams pass through polarizer P_2 and lens L_2 focuses them onto a microscope objective MO, and the resulting interferometric pattern is detected by a CCD. The dashed lines around QWP_1 indicate that it is used in some cases and not in others.

can be used to estimate the $XYZW$ parameters. It was heuristically determined. It was found that at least eight measurements that *properly mix* all the parameters are needed. It was tested (not shown) that applying the least squares method to the Moreno measurements does not give smooth and noiseless results. Moreover, it was tested (not shown) that increasing the number of measurements in the least squares method (for example, by including some of the complementary measurements) does not improve the results. In the next section, the LCD characterization is completed by measuring its global phase to employ it as a phase-mostly spatial light modulator.

5. GLOBAL PHASE MEASUREMENT

In this section, the global phase β [see Eq. (2)] is determined. The procedures of Moreno *et al.* [14] and Ma *et al.* [15] are followed closely. To this end, the setup shown in Fig. 3 was employed. A spatially filtered and collimated laser beam is polarized by P_1. This beam impinges onto the LCD, which has a pupil with two holes. Over one aperture the gray level is fixed ($gl = 0$) and in the other the gray level is varied. The light coming from both apertures passes through another polarizer P_2 and then is focused by lens L_2. The resulting interferogram is then recorded by means of the microscope-objective–CCD array.

The intensity resulting from each aperture is described by

$$\tilde{I}(\theta_1, \theta_2) = (X\cos(\theta_1 - \theta_2) + Z\sin(\theta_1 - \theta_2))^2 + (Y\cos(\theta_1 + \theta_2) + W\sin(\theta_1 + \theta_2))^2. \quad (12)$$

Recall that θ_1 and θ_2 are the angles of the polarizers P_1 and P_2, respectively. Assuming the total phase difference between the field belonging to each aperture is described by a phasor term of the form $\exp(-j\delta)$, the global phase can be written as

$$\beta = \delta - \arctan\left(\frac{Y\cos(\theta_1 + \theta_2) + W\sin(\theta_1 + \theta_2)}{X\cos(\theta_1 - \theta_2) + Z\sin(\theta_1 - \theta_2)}\right). \quad (13)$$

In order to have a good contrast of the interference fringes while performing the measurement, the minimum intensity variation is needed across all gray levels. Then, the angles $\theta_{1_{\min}}$ and $\theta_{2_{\min}}$, which minimize the intensity variation, were determined by minimizing

$$p(\theta_1, \theta_2) = \frac{\mathrm{Max}[\tilde{I}(\theta_1, \theta_2)] - \mathrm{Min}[\tilde{I}(\theta_1, \theta_2)]}{\mathrm{Max}[\tilde{I}(\theta_1, \theta_2)]}, \quad (14)$$

where Max/Min are calculated over all the gray levels. The minimization was also performed with the Nelder–Mead method included in the `NMinimize` package of Wolfram Mathematica [21,22] (a Wolfram Mathematica implementation of this optimization can be downloaded from [23]).

Once the angles were determined ($\theta_{1_{\min}} = 11.5°$, $\theta_{2_{\min}} = 55.7°$), the intensity was directly measured with the CCD and the phase was determined by standard methods [26].

Figure 4 presents the results of this section. The measured intensity (normalized to the maximum) along with that calculated by means of Eq. (12) are depicted in Fig. 4(a). A clear correspondence is observed between them. Then, once again, the correctness of the prediction of the least squares method is verified. Figure 4(b) shows the results of measuring the total phase δ and of calculating the global phase β. From this figure it is clear that, for the polarizer angles considered, the main contribution for the total phase is given by β, although the Jones matrix can add a phase of the order of π for other angles. This step completes the LCD characterization. In the next section, the full characterization of our LCD is employed to obtain a phase-mostly configuration.

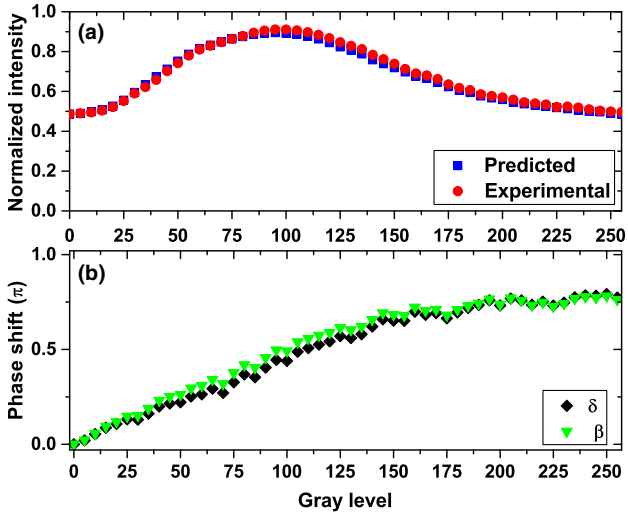

Fig. 4. (a) Predicted and experimental results for the intensity with $\theta_1 = 11.5°$ and $\theta_2 = 55.7°$. (b) Measured δ and calculated β with the configuration of part (a).

6. PHASE-MOSTLY CONFIGURATION

One of the main uses of LCDs in all optic laboratories is as a phase-mostly spatial light modulator. This is accomplished by placing the LCD between two polarizers and adding at least one quarter-wave plate between them. In our case, as in the characterization method, we use only one wave plate before the LCD. To determine the proper angles to be set in the optical components, it is necessary to perform a phase and amplitude optimization. Here, in a similar way to that in Section 5, and closely follow the Moreno *et al.* [14] and Ma *et al.* [15] procedures, two parameters are defined as

$$q(\theta_1, \phi, \theta_2) = \frac{\mathrm{Max}[I(\theta_1, \phi, \theta_2)] - \mathrm{Min}[I(\theta_1, \phi, \theta_2)}{\mathrm{Max}[I(\theta_1, \phi, \theta_2)]}, \quad (15)$$

$$r(\theta_1, \phi, \theta_2) = \mathrm{Max}[\varphi(\theta_1, \phi, \theta_2)] - \mathrm{Min}[\varphi(\theta_1, \phi, \theta_2)], \quad (16)$$

where again Max/Min are calculated over all the gray levels, $I(\theta_1, \phi, \theta_2)$ is given by Eq. (9), and

$$\begin{aligned}\varphi(\theta_1, \phi, \theta_2) = \arctan[&(X\cos(\theta_1 - \theta_2) - Y\cos(\theta_1 - \theta_2 - 2\phi)\\ &+ Z\sin(\theta_1 - \theta_2)\\ &+ W\sin(\theta_1 - \theta_2 - 2\phi))/(X\cos(\theta_1 + \theta_2 - 2\phi)\\ &+ Y\cos(\theta_1 + \theta_2) - Z\sin(\theta_1 + \theta_2 - 2\phi)\\ &+ W\sin(\theta_1 + \theta_2))] + \beta. \end{aligned} \quad (17)$$

Then, the optimization is carried out by searching for the minimum value of q/r. It has to be stressed that by minimizing this quotient, the intensity variation is minimized and the phase modulation is maximized, simultaneously. Once again, the Nelder–Mead method included in the `NMinimize` package of Wolfram Mathematica is employed for the optimization [21,22] (a Wolfram Mathematica implementation of this optimization can be downloaded from [23]). Due to the complexity of the search, a mesh with 25 initial points per variable is considered.

The optimization procedure gives $\theta_{1_{\mathrm{pm}}} = 96.7°$, $\phi_{\mathrm{pm}} = 29.9°$, and $\theta_{2_{\mathrm{pm}}} = 68.5°$ with a maximum phase modulation of 1.57π and a coupled intensity (normalized to the maximum) of 1.5%. The average transmittance of this configuration is 67%, which shows that it is possible to obtain a phase-mostly modulation with a reasonably high transmittance.

To confirm the predicted result, an experimental setup like the one shown in Fig. 3 was implemented and in this case the QWP was employed. The intensity and phase were measured as in previous sections. Figure 5 presents the measured values along with the prediction obtained with the optimized angles. As an overall comment, good agreement between the points is apparent. As can be seen for the phase modulation, the optimized curve closely follows the experimental one, although the maximum modulation obtained experimentally is lower than the predicted one. In the experimental case, the maximum modulation achieved was 1.49π. On the other hand, for the normalized intensity, it can be seen that the measured intensity narrowly matches the predicted one, but it depart slightly for $gl < 30$ (the experimental coupled intensity is around 4%). This difference together with the lower phase modulation measured could be explained by the low resolution of the optical components. In particular, the QWP has a minimum scale of 2°, which limits the possibility of properly setting its angle. However, it is clear that the least squares method combined with the measurement of the global phase and an optimization procedure allows one to achieve a phase-mostly regime with high phase modulation and high intensity transmittance.

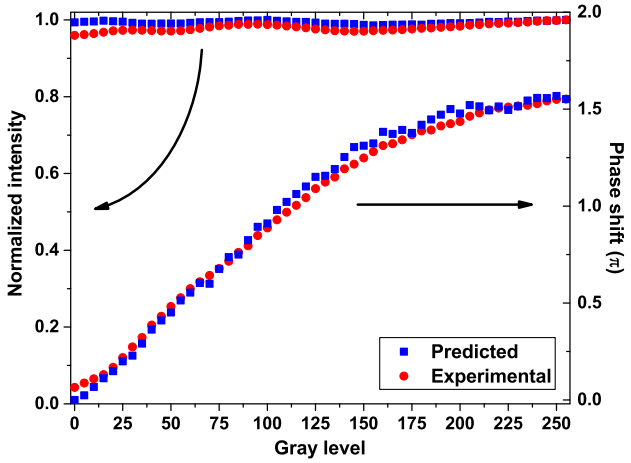

Fig. 5. Predicted and experimental results for phase-mostly modulation. The angles were set to $\theta_1 = 96.7°$, $\phi = 29.9°$, and $\theta_2 = 68.5°$.

7. CONCLUSION

In this work, a method for liquid crystal display characterization has been presented. This method is based on the assumption that an LCD can be considered as a polarization-changing device and it is well described by a Jones matrix and a global phase. The Jones matrix parameters are found by a least squares minimization based on the optimization algorithm of the Nelder–Mead method included in the `NMinimize` package of Wolfram Mathematica. The effectiveness of this optimization was revealed by calculating the predicted intensities employed for the implementation comparing them with the very similar experimental measurements. The present method overcomes the drawbacks and misconceptions appearing in previous ones, i.e., avoids the need for assigning experimental values to theoretical expressions, it is robust against intensity fluctuations, does not need to arbitrarily fix any sign of the estimated parameters, and only one quarter-wave plate is employed. These facts have been exposed by a revision of previous methods and explicitly demonstrated by a comparative analysis of the results obtained for each one. Once the Jones matrix parameters were obtained, the global phase was determined and a phase-mostly configuration was obtained and experimentally verified.

It must be highlighted that the eight intensity measurements were heuristically determined. This should not be seen as a weakness but as the ability to customize the method. Recall that it was found that at least eight measurements that *properly mix* all the parameters are needed. In this sense, other measurements could be performed according to the needs of the experimenter. For example, the method could be implemented with the QWP behind the LCD. This flexibility reveals the strength of the least squares method.

Finally, it has to be stressed that this method can be applied to any nonabsorbing linear polarization device that can be described by a Jones matrix. Besides, it can help other approaches, such as those related to the Jones matrix of an LCD with an equivalent system composed of a rotator followed by a linear retarder [27,28].

APPENDIX A: DETAILED ANALYSIS OF FIG. 2

From Fig. 2(a), note that I_6 is very similar to I_7, suggesting that $W \approx 0$ [see Eqs. (4f) and (4g)]. However, when calculating W from Eq. (5d), it gives values well differentiated from zero for $gl > 180$ as can be seen in Fig. 2(d). This behavior appears because I_2 amplifies the differences between the quotients of $(I_5 - I_7)$ and $(I_3 - I_4)$ and the crossing of I_3 and I_4 at $gl \approx 180$, which contributes to the sign change of W [see Eq. (6b)]. In the cases of X and Y, they appear noisy in the range of $15 < gl < 40$ as a consequence of $I_3 \approx I_4$ for $gl < 40$ and they cross at $gl \approx 35$ [see Eqs. (5a) and (5b)]. Additionally, I_6 and I_7 cross at $gl \approx 20$, which contributes to the noise and to the abrupt sign change of Y as deduced from Eq. (6a). In a similar way, the crossing of I_6 and I_7 at $gl \approx 180$ contributes to the noise of X and Y and to the abrupt sign change of Y.

On the other hand, from Fig. 2(b) it is clear that for $gl > 200$, I_1', and I_3' are very close to zero, whereas I_2' is noticeably less than one. For this reason, when attempting to calculate X from Eq. (8a), this expression takes a negative value and its square root gives an imaginary result, which is nonsense. Consequently, for $gl > 200$ the X parameter is undetermined, as shown in Fig. 2(e). Something similar happens with Z and W. In the case of Z, from Fig. 2(b) it is notorious that for $gl < 45$, I_2' is less than I_1' and I_3' is near one. Then, when Eq. (8c) is employed, nonreal values are found for $gl < 45$, leaving Z ill-defined. For the case of W, it can be seen that the difference $I_1' - I_3'$ is larger than $1 - I_2'$ for $70 < gl < 170$, which again results in imaginary nonsense values.

APPENDIX B: ANALYSIS OF DEPOLARIZATION ERROR

Assuming that the light coming from the LCD is composed of a polarized component I and a unpolarized contribution Δ, the error of measuring a normalized intensity is given by

$$\text{error} = \frac{I + \frac{\Delta}{2}}{1 + \Delta} - I, \tag{B1}$$

where the first term correspond to the normalized intensity measured without accounting for depolarization, whereas the second term represents the correct measurement. Figure 6 shows this error as a function of the depolarization component for several values of intensity. It is apparent that the error is symmetrically distributed around zero for intensities in the interval [0,1] being exactly zero for $I = 0.5$. Note that for a 10% of depolarized component, the error in the measured intensity is less than 5%.

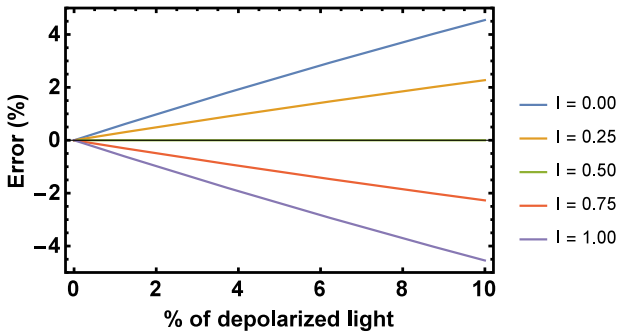

Fig. 6. Analysis of the error of measuring the light coming from an LCD without considering depolarization.

Funding. Proyectos de Investigación Plurianuales (PIP-CONICET) (0549); Universidad Nacional de La Plata (UNLP) (11/I168).

Acknowledgment. D. G. Actis acknowledges CICBA for the *Beca de Entrenamiento*. D. Amaya thanks CONICET for the post-doctoral fellowship.

REFERENCES

1. A. L. Gaunt, T. F. Schmidutz, I. Gotlibovych, R. P. Smith, and Z. Hadzibabic, "Bose–Einstein condensation of atoms in a uniform potential," Phys. Rev. Lett. **110**, 200406 (2013).
2. L. Zhao, X. Guo, Y. Sun, Y. Su, M. M. T. Loy, and S. Du, "Shaping the biphoton temporal waveform with spatial light modulation," Phys. Rev. Lett. **115**, 193601 (2015).
3. L. Cabezas, D. Amaya, N. Bolognini, and A. Lencina, "One dimensional speckle fields generated by three phase level diffusers," J. Opt. **17**, 025602 (2015).
4. L. Cabezas, D. Amaya, N. Bolognini, and A. Lencina, "Speckle fields generated with binary diffusers and synthetic pupils implemented on a spatial light modulator," Appl. Opt. **54**, 5691–5696 (2015).
5. E. Rueda, D. Muñetón, J. A. Gómez, and A. Lencina, "High-quality optical vortex-beam generation by using a multilevel vortex-producing lens," Opt. Lett. **38**, 3941–3944 (2013).
6. N. Londoño, E. Rueda, J. A. Gómez, and A. Lencina, "Generation of optical vortices by using binary vortex producing lenses," Appl. Opt. **54**, 796–801 (2015).
7. P. Vaveliuk, A. Lencina, J. A. Rodrigo, and O. Martnez-Matos, "Intensity-symmetric airy beams," J. Opt. Soc. Am. A **32**, 443–446 (2015).
8. P. Vaveliuk, A. Lencina, J. A. Rodrigo, and O. M. Matos, "Symmetric airy beams," Opt. Lett. **39**, 2370–2373 (2014).
9. L. Vicari, *Optical Applications of Liquid Crystals* (CRC Press, 2016).
10. B. E. A. Saleh and K. Lu, "Theory and design of the liquid crystal TV as an optical spatial phase modulator," Opt. Eng. **29**, 240–246 (1990).
11. A. Márquez, J. Campos, M. J. Yzuel, I. Moreno, J. A. Davis, C. Iemmi, A. Moreno, and A. Robert, "Characterization of edge effects in twisted nematic liquid crystal displays," Opt. Eng. **39**, 3301–3307 (2000).
12. J. A. Coy, M. Zaldarriaga, D. F. Grosz, and O. E. Martínez, "Characterization of a liquid crystal television as a programmable spatial light modulator," Opt. Eng. **35**, 15–19 (1996).
13. M. Yamauchi, "Jones-matrix models for twisted-nematic liquid-crystal devices," Appl. Opt. **44**, 4484–4493 (2005).
14. I. Moreno, P. Velásquez, C. R. Fernández-Pousa, M. M. Sánchez-López, and F. Mateos, "Jones matrix method for predicting and optimizing the optical modulation properties of a liquid-crystal display," J. Appl. Phys. **94**, 3697–3702 (2003).
15. B. Ma, B. Yao, T. Ye, and M. Lei, "Prediction of optical modulation properties of twisted-nematic liquid-crystal display by improved measurement of jones matrix," J. Appl. Phys. **107**, 073107 (2010).
16. F. P. Ferreira and M. S. Belsley, "Direct calibration of a spatial light modulator by lateral shearing interferometry," Opt. Express **18**, 7899–7904 (2010).

17. V. Duran, J. Lancis, E. Tajahuerce, and V. Climent, "Poincaré sphere method for optimizing the phase modulation response of a twisted nematic liquid crystal display," J. Disp. Technol. **3**, 9–14 (2007).
18. T. Khos-Ochir, P. Munkhbaatar, B. K. Yang, H. W. Kim, J. S. Kim, and M.-W. Kim, "Polarimetric measurement of Jones matrix of a twisted nematic liquid crystal spatial light modulator," J. Opt. Soc. Korea **16**, 443–448 (2012).
19. A. Arias, private communication (forwarded email from Baoli Yao), August 8, 2013.
20. W. H. Press, S. A. Teukolsky, W. T. Vetterling, and B. P. Flannery, *Numerical Recipes in C* (Cambridge University, 1992).
21. J. A. Nelder and R. Mead, "A simplex method for function minimization," Comput. J. **7**, 308–313 (1965).
22. E. W. Weisstein, "Nelder–Mead Method," MathWorld–A Wolfram Web Resource, 2016, http://mathworld.wolfram.com/Nelder-MeadMethod.html.
23. D. Amaya, D. G. Actis, G. Rumi, and A. Lencina, "Jones Matrix Parameters-Least Squares Method-V1.0.nb," Figshare.com, 2016.
24. A. Márquez, I. Moreno, C. Iemmi, A. Lizana, J. Campos, and M. J. Yzuel, "Mueller–Stokes characterization and optimization of a liquid crystal on silicon display showing depolarization," Opt. Express **16**, 1669–1685 (2008).
25. I. Moreno, A. Lizana, J. Campos, A. Márquez, C. Iemmi, and M. J. Yzuel, "Combined Mueller and Jones matrix method for the evaluation of the complex modulation in a liquid-crystal-on-silicon display," Opt. Lett. **33**, 627–629 (2008).
26. M. Takeda, H. Ina, and S. Kobayashi, "Fourier-transform method of fringe-pattern analysis for computer-based topography and interferometry," J. Opt. Soc. Am. **72**, 156–160 (1982).
27. V. Durán, J. Lancis, E. Tajahuerce, and Z. Jaroszewicz, "Equivalent retarder-rotator approach to on-state twisted nematic liquid crystal displays," J. Appl. Phys. **99**, 113101 (2006).
28. C.-J. Yu, Y.-T. Tseng, K.-C. Hsu, and C. Chou, "Full-field characterization of a twisted nematic liquid-crystal device using equivalence theorem of a unitary optical system," Appl. Opt. **51**, 238–244 (2012).

186.65.183.71 {ts '2017-02-07 12:19:01'}